Preprint of

Tailoring the Optimal Control Cost Function to a Desired Output: Application to Minimizing Phase Errors in Short Broadband Excitation Pulses

T. E. Skinner, T. O. Reiss, B. Luy, N. Khaneja, S. J. Glaser

J. Magn. Reson. 172, 17-23 (2005).

EDITOR'S HIGHLIGHTED VERSION
NEW TITLE:
Tailoring the cost function to performance in optimal control theory

Thomas E. Skinner,[a,*] Timo O. Reiss,[b] Burkhard Luy,[b] Navin Khaneja,[c] Steffen J. Glaser,[b]

[a] *Physics Department, Wright State University, Dayton, OH 45435, USA*
[b] *Institut für Organische Chemie und Biochemie II, Technische Universität München, Lichtenbergstr. 4, 85747 Garching, Germany*
[c] *Division of Engineering and Applied Sciences, Harvard University, 29 Oxford Street, Cambridge, MA 02138, USA*

[*] *Corresponding author. Fax: 1-937-775-2222*
E-mail: thomas.skinner@wright.edu, glaser@ch.tum.de

Received ; revised ; accepted .

[[**NEW ABSTRACT:**]] **The de facto standard cost function has been used heretofore to characterize the performance of pulses designed using optimal control theory. The freedom to choose new, creative quality factors designed for specific purposes is demonstrated. The utility of the current approach is most clearly illustrated by comparison to previous applications—specifically, broadband excitation. The resulting pulses are limited to the same maximum RF amplitude used previously and tolerate the same variation in RF homogeneity deemed relevant for standard high-resolution NMR probes. Design criteria, again, are transformation of $I_z \rightarrow I_x$ over resonance offsets of ± 20 kHz and RF variability of $\pm 5\%$, with a peak RF amplitude equal to 17.5 kHz. Compared to previous broadband excitation by optimized pulses (BEBOP), significantly shorter pulses are achievable, with only marginally reduced performance. Simulations transform I_z to greater than 0.98 I_x, with phase deviations of the final magnetization less than 2°, over the targetted ranges of resonance offset and RF variability. Experimental performance is in excellent agreement with the simulations. The new cost effectively trades a small increase in residual z magnetization for improved phase in the transverse plane at shorter pulse lengths.**

Key Words: broadband excitation, BEBOP, optimal control theory.

INTRODUCTION

[[**The nearly ideal performance of pulses obtained using optimal control theory [1, 2, 3, 4, 5, 6] provides a strong inducement for developing further the capabilities of this very general and flexible methodology. The goal is to characterize the performance of optimal control algorithms for use in general NMR applications. Excitation is a particularly simple example that allows a clear delineation between the effects of optimal control and the application, which might be less apparent with a more complicated sequence. Requiring dual compensation for RF inhomogeneity/miscalibration and chemical shift variation, a historically difficult challenge for other methodologies [7, 8, 9, 10, 11, 12, 13, 14, 15, 16, 17, 18, 19], provides siginificant additional relevance.**]]

In our initial algorithm for implementing the theory, the maximum amplitude of the RF controls was constrained indirectly—a given pulse length (2 ms) and convergence factor for terminating the algorithm resulted in a maximum pulse amplitude of 17.5 kHz. [[**This first application of optimal control to broadband excitation**]] [4] was shown to excite transverse magnetization of nearly constant phase over resonance offsets of 40 kHz with up to 4 dB tolerance to RF miscalibration. Direct control of peak RF amplitude was subsequently provided by clipping the RF at a desired peak value, forcing the optimal control algorithm to search in a different direction whenever it obtained an amplitude that exceeded the limit. This allowed us to reduce pulse length to 500μs and yet still

significantly improve pulse performance over the targetted ranges of RF and resonance offset variation [5].

We now consider the effect of modifying the cost function used to characterize the performance of a pulse in the optimization. Previously, this cost was measured by projecting the magnetization vector at the end of the pulse onto the target state. [[**This projection of a final state achieved by the controls onto the target state is very general. For example, the states could be Schrödinger wave functions in a different type of application. But we note that projection (and a closely related form, the magnitude of the difference between the final state and the target) is virtually the only cost function employed in a wide range of optimization protocols.**]] Maximizing this projection minimizes the cone angle between the final magnetization and the target state. This particular cost function therefore requires small cone angles to ensure the phase of the final magnetization in the transverse plane has the same small value, which means the alignment between target and final states has to be almost perfect. The level of perfection achieved so far is not possible if the pulse length is too short. However, the residual z component of the final magnetization has no effect on the phase of the NMR spectrum. One could therefore anticipate that allowing a larger cone angle in the z direction while maintaining the small cone angle in the transverse plane might provide acceptable performance with shorter pulses. [[**The utility of this new approach is demonstrated specifically by the design of a 125 μs broadband excitation pulse, compensated for RF inhomogeneity, with outstanding performance characteristics. More importantly, we emphasize the wider utility of alternative cost functions in general applications of optimal control theory.**]]

THEORY AND METHODS

Details of the optimal control procedure, as it relates to broadband excitation in NMR, are discussed in [4]. Further general information on broadband excitation [7, 8, 9, 10, 11, 12, 13, 14, 15, 16, 17, 18, 19], optimal control theory [20, 21, 22, 23], and its use in NMR [1, 2, 3] is provided in the references. In this section, we consider the modifications to our previous treatment associated with the new cost function.

Optimal Control Theory: A New Cost Function for Excitation

During the time interval $[t_0, t_p]$, we seek to transfer initial magnetization $\boldsymbol{M}(t_0) = \hat{\boldsymbol{z}}$ to the target final state $\boldsymbol{F} = \hat{\boldsymbol{x}}$ for a specified range of chemical-shift offsets and a desired degree of tolerance to RF inhomogeneity or miscalibration. The trajectories $\boldsymbol{M}(t)$ are constrained by the Bloch equation

$$\dot{\boldsymbol{M}} = \boldsymbol{\omega}_e \times \boldsymbol{M}. \tag{1}$$

The effective RF field $\boldsymbol{\omega}_e$ in angular frequency units (radians/sec) can be written in the rotating frame as

$$\boldsymbol{\omega}_e = \omega_1(t)\,[\cos\phi(t)\,\hat{\boldsymbol{x}} + \sin\phi(t)\,\hat{\boldsymbol{y}}\,] + \Delta\omega(t)\,\hat{\boldsymbol{z}}, \tag{2}$$

which encompasses any desired modulation of the amplitude ω_1, phase ϕ, and frequency offset $\Delta\omega$ of the pulse. As in our previous work, only amplitude and phase modulation are considered, since typical spectrometers implement frequency modulation as a phase modulation, with $\Delta\omega(t) = d\phi(t)/dt$. The value of $\Delta\omega$ is therefore time-independent, and gives the chemical shift of the irradiated spin.

Constraints on the optimization can be effectively incorporated into the formalism using the technique of Lagrange multipliers (see for example, [24]). The vector Bloch equation thus introduces a vector Lagrange multiplier $\boldsymbol{\lambda}$. Some suitable measure of pulse performance, the cost function Φ, is then defined as the object of the optimization. The necessary conditions that must be satisfied at each time for the cost to be optimized are

$$\dot{\boldsymbol{M}} = \boldsymbol{\omega}_e \times \boldsymbol{M}, \qquad \boldsymbol{M}(t_0) = \hat{\boldsymbol{z}} \tag{3}$$

$$\dot{\boldsymbol{\lambda}} = \boldsymbol{\omega}_e \times \boldsymbol{\lambda}, \qquad \boldsymbol{\lambda}(t_p) = \partial\Phi/\partial\boldsymbol{M} \tag{4}$$

$$\boldsymbol{M} \times \boldsymbol{\lambda} = 0 \tag{5}$$

Thus, both $\boldsymbol{M}$ and $\boldsymbol{\lambda}$ obey the Bloch equation. Since $\boldsymbol{\omega}_e(t)$ controls the evolution of $\boldsymbol{M}(t)$, the goal of finding the optimum trajectory is the same as finding the optimal RF sequence to apply to the sample. The particular choice of the dot product $\Phi = \boldsymbol{M}(t_p) \cdot \boldsymbol{F}$ used previously for the cost quantifies the degree to which $\boldsymbol{M}(t_p) = \boldsymbol{F}$ and gives $\boldsymbol{\lambda}(t_p) = \boldsymbol{F}$. As noted previously [4], there is a simple geometrical interpretation for this case. A sequence which transforms $\boldsymbol{M}(t_0)$ forward in time to the desired target state $\boldsymbol{F}$ therefore transforms $\boldsymbol{\lambda}(t_p) = \boldsymbol{F}$ backwards in time to $\boldsymbol{M}(t_0)$. For the optimal pulse, we then have $\boldsymbol{M}_{\rm opt}(t) = \boldsymbol{\lambda}_{\rm opt}(t)$, which satisfies the stationary condition given by Eq. [5].

This cost defines a cone of possible final states $\boldsymbol{M}(t_p)$ centered on the x axis with vertex at the origin, all weighted equally. We were forced to obtain small cone angles to ensure the phase in the transverse plane has the same small value, which means the excitation efficiency has to be almost perfect. If, for example, $M_x = 0.95M_0$, which is a reasonably high excitation efficiency, an unacceptable phase of $\sim 18°$ results if the final magnetization lies entirely in the transverse plane. Changing the cost so that it favors final states oriented in the xz plane would allow $M_x = 0.95M_0$ with a transverse (i.e., spectral) phase of $0°$. This could be achieved by minimizing the magnitude of the residual vector, $||\boldsymbol{M} - \boldsymbol{F}||^2$, with appropriate weighting for each component. We therefore consider a cost of the form

$$\Phi = \sum_{i=1}^{3} a_i (M_i - F_i)^2. \tag{6}$$

For the desired target along the x axis, a weight of zero for the z component and equal weights for the other two components allows the optimal control algorithm the flexibility to do anything it wants with the z component as long as M_x is maximized and M_y minimized.

We now have, according to Eq. [4],

$$\lambda_i(t_p) = 2\, a_i(M_i - F_i), \tag{7}$$

with the factor of 2 representing a scaling that can be absorbed in the weights a_i. Since $\boldsymbol{\lambda}(t_p)$ now depends on the final state $\boldsymbol{M}$, which, in turn, depends on the RF pulse applied, a physical interpretation for the optimal control process is not as straightforward as for the previous cost function. Nonetheless, the procedure is still the same—$\boldsymbol{M}$ and $\boldsymbol{\lambda}$ obey the Bloch equation, and they can be calculated at each time for a given pulse. $\boldsymbol{M}_{\rm opt}(t)$ will satisfy the stationary condition of Eq. [5] when $\boldsymbol{\lambda}_{\rm opt}(t) = 0$. For a nonoptimal pulse, $\boldsymbol{M} \times \boldsymbol{\lambda}$ at each time point of the two trajectories gives the proportional adjustment to make in the control field $\boldsymbol{\omega}_e(t)$.

Numerical Algorithm

There is no change to the basic algorithm for optimizing the cost and incorporating the RF clipping procedure specifying that the amplitude at each time, $\omega_1(t)$, be no greater than a chosen maximum amplitude $\omega_{\rm max}$. [[**It is provided here for convenience:**]]

i) Choose an initial RF sequence $\boldsymbol{\omega}_e^{(0)}$.

ii) Evolve $\boldsymbol{M}$ forward in time from the initial state $\hat{\boldsymbol{z}}$.

iii) Calculate $\boldsymbol{M}(t_p) \times \boldsymbol{\lambda}(t_p)$ and evolve it backwards in time.

iv) $\boldsymbol{\omega}_e{}^{(k+1)}(t) \rightarrow \boldsymbol{\omega}_e{}^{(k)}(t) + \epsilon\,[\,\boldsymbol{M}(t) \times \boldsymbol{\lambda}(t)\,]$

v) For any $\omega_1(t) > \omega_{\rm max}$, set $\omega_1(t) \rightarrow \omega_{\rm max}$.

vi) Repeat steps ii)–v) until a desired convergence of Φ is reached.

The RF clipping in step v) is implemented by adjusting $(\omega_1)_x$ and $(\omega_1)_y$ to satisfy the constraint on maximum RF amplitude without changing the phase of ω_1. Additional details concerning each step and adjustments related to the demands of broadband excitation are described in [4, 5].

RESULTS AND DISCUSSION

[[**The emphasis of this work is the continued development of productive modifications to the basic optimal control algorithm. We feel this provides the most general applicability of the methodology. Since productivity is relative and assessed by comparison, we first summarize our previous results. We then provide steps leading to the current result, including details relevant for researchers interested in pursuing their own applications. The results and their implications conclude the section.**

In all the pulses pertinent to the present discussion, optimal control was applied over resonance offsets of ± 20 kHz, with a variation of $\pm 5\%$ in the nominal RF calibration. The pulses were typically digitized in 0.5μs increments. In developing our first broadband excitation pulse]] [4], there was no explicit control of the peak RF amplitude. The pulse length and convergence parameter for terminating the algorithm were set sufficiently large that acceptable performance was obtained without exceeding the power limits of typical ^{13}C probes. We obtained a 2 ms pulse with maximum RF amplitude equal to 17.5 kHz capable of transforming 99.5% of initial z magnetization, M_0, to within 4° of the x axis over the targetted RF and offset ranges. By implementing the clipping algorithm [5], we then obtained a 500 μs pulse (17.5 kHz peak RF) with the same, almost perfect, excitation efficiency and even smaller residual phase of less than 2° over the optimized ranges. Moreover, the performance of this second pulse exceeds the design criteria, providing an outstanding 99% excitation efficiency over almost a $\pm 15\%$ variation in nominal RF, with the maximum phase of the final magnetization still less than $\sim 4°$ over this larger RF range, operating over the same 40 kHz bandwidth.

We next searched for a 125μs pulse. Using a random initial waveform, as in the previous procedures, and the original cost function, $\boldsymbol{M} \cdot \boldsymbol{F}$, provided a pulse giving at least 95% excitation with phase less than 5° over the optimization window. This is fairly good performance, but it is rather poor compared to our previous pulses. We therefore tried a new method, in the expectation that it might give the algorithm additional flexibility in finding an optimal solution. We first used a random initial waveform, digitized in 4000 points, together with the original cost function to obtain a 125μs pulse with an average excitation of 99.6% over the targetted optimization ranges. Although this pulse, at ~ 30 nanosec per time step, may not be very practical from the standpoint of actual implementation, it provides the seed for finding pulses with reduced digitization. Every other point of this pulse is used as the initial input to the algorithm to generate a pulse with half the digitization. Every other point of this resulting pulse is then used as a new initial input. Proceeding in this manner, we obtained a 250-point 125μs pulse maintaining the same value of 99.6% for the average excitation. However, this average includes values as low as 98% and phases as high as 12° in the optimization window.

We also tried using the 500μs BEBOP as a "breeder" for shorter pulses. As before, we used every other point of this pulse as the initial waveform, but also shortened the pulse length to 250μs, still employing the original cost function. Somewhat surprisingly, this new pulse provides almost the same, practically ideal, performance as the 500μs pulse. If we continue in this manner, using every other point of the 250μs pulse to generate a 125μs pulse, we find it provides

better than 98% excitation over the RF and offset optimization ranges, but the phase can be as high as 10° at the lower extreme of the RF range.

Although the performance of the two 125μs pulses obtained using our original cost function is very good, better phase performance would be desirable, if possible. We therefore adopted the new cost function of Eq. [6], weighted according to $\boldsymbol{a} = (1, 1, 0)$, as discussed in the previous section. These values for the weights gave the best performance compared to an assortment of other possibilities that were tried, but our list was by no means exhaustive, and other combinations may be useful. Both of the 125μs pulses obtained to that point were tried as initial waveforms, as well as many others. The 125μs descendant of the 500μs pulse, as just described, ultimately generated the best performance when fed to the algorithm employing the new cost function. We also used this new 125μs pulse (generated using the new cost function) as input to our procedure for developing pulses of decreased digitization to obtain a 125μs pulse digitized in 7.8μs increments (16 time steps).

The amplitude and phase of these 125μs BEBOP pulses are plotted as a function of time in Fig. 1 for comparison with our earlier pulses. The somewhat anticipated outcome is that shortening the pulse length sufficiently in conjunction with the clipping algorithm has finally forced the optimal control procedure to maximize RF amplitude, approaching a pure phase modulated pulse. The progression in pulse development is shown for the original cost function (panel A), the new cost function (panel B), and decreased digitization using the new cost (panel C).

The theoretical performance of the pulse in Fig. 1B, assuming simple Bloch equation evolution of the irradiated spins (as in the optimization procedure), is illustrated in Fig. 2. Contours of x magnetization, M_x, are plotted in the upper panel as functions of resonance offset and RF inhomogeneity. The phase of the excited magnetization is shown similarly in the lower panel. Over the targetted ±5% variation in the nominal RF delivered by the coil and resonance offsets of ±20 kHz, the excited magnetization M_x is better than 98% of the initial z magnetization, M_0, with a phase of less than 2°. A similar plot (not shown) for the 16-point pulse of Fig. 1C shows 97% excitation with phase of less than 3° over these same ranges of RF and offset varation.

Magnetization in the range 0.97–0.98 M_0 would have a phase of 12–14° if it was entirely in the transverse plane, so the new cost function is highly effective. It provides the capability to allow slightly reduced excitation efficiency without increasing the phase to unacceptable levels. A more precise comparison is provided in Fig. 3, showing the location of the final magnetization in the y-z plane for both the original and the new cost functions. The new cost narrows the y distribution significantly at the expense of a small increase in width of the z distribution.

Figure 4 shows the experimental performance of the pulses in Fig. 1B,C. They are in excellent agreement with the simulations. The calibrated pulse at 0 dB (17.5 kHz peak RF) and pulses applied with attenuations of ±0.5 dB ($-5.6\%, +5.9\%$) relative to the calibrated RF values match the nearly ideal performance discussed previously for the simulations. At ±1 dB ($-10.9\%, +12.2\%$), the pulses still provide tolerable performance, with $M_x > 0.95$ and a phase less than 4° within the 40 kHz offset range.

In contrast to the longer pulses developed previously, the pulse length is now sufficiently short that the best performance of these pulses does not extend significantly beyond the optimization window. A detailed analysis of both excitation and inversion efficiency as a function of pulse length [6] shows a steep drop in performance below a minimum pulse length (depending on the parameters defining the optimization), and this is indeed the case here. The best 100μs pulses we obtain provide, respectively, 95% excitation with 6° phase and 93% excitation with 2–3° phase. We also obtained a 62.5μs pulse giving 90% excitation with 3° phase.

The benchmark for comparing pulse performance in previous work [4, 5] required at least 95% excitation efficiency and a phase roll of no more than 4° over the resonance offset range. We used the standard definition for figure-of-merit (FOM) as the total excitation bandwidth satisfying the benchmark divided by the peak RF amplitude. The 100μs BEBOP thus represents a conservative lower limit on pulse length for achieving FOM = 2.3 with tolerance of ±5% in RF calibration.

EXPERIMENTAL

DELETED (since there is now virtually no amplitude modulation): [[BEBOP requires accurate RF output from system hardware. However, we have not found the rapid changes in pulse amplitude to be a problem for modern NMR consoles. Details of our procedures for ensuring the fidelity of console output have been described previously [4, 5].]]

Experimental excitation profiles were implemented on a Bruker DMX 900 spectrometer equipped with modern SGU units for RF control and linearized amplifiers. A sample of 99.96 % D_2O was doped with $CuSO_4$ to a final T_1 relaxation time of ∼500 ms. To reduce effects of B_1-field inhomogeneity, approximately 40 μl of this solution was placed in a Shigemi limited volume tube. The maximum RF amplitude was calibrated using a square shaped pulse. Offset profiles were obtained by varying the offset of the shaped pulses from -27000 Hz to 27000 Hz in steps of 1000 Hz. In order to also monitor the B_1-field dependence of the pulses, the experiments were repeated with ±0.5 and ±1 dB attenuation relative to the calibrated RF

amplitude, corresponding to maximum RF fields of 15597, 16521, 17500, 18537, and 19635 Hz. The results are shown in Fig. 4 with the theoretical magnitude of M_x after excitation drawn on top of the individual offset profiles. The experimental data provide an excellent match with theory.

The offsets were implemented by superimposing a linear phase ramp on the shaped pulse. For pulses digitized in sufficiently small increments, the phase increment per time step is small, so this smoothly changing phase provides a good approximation of a constant frequency offset. However, for the 16-point 125μs pulse of Fig. 1C, the phase increment per time step gives too large a jump to accurately represent the frequency offset. Digitization artifacts are not negligible compared to pulses digitized in much smaller time steps. The 16-point pulse was therefore represented using 256 points, allowing the phase ramp to be more accurately realized. We commented in [5] that a 500 μs pulse derived with reduced digitization displayed slight differences between theory and experiment, especially at high frequency offsets. We suggested that the differences between simulation and experiment were likely due to the implementation of the offset profiles. The current implemention eliminates those differences.

CONCLUSION

[[The cost function provides the necessary measure for assessing the degree to which the goals of an optimization have been met. Although a standard cost function is typically employed in the field of optimization, it is not the only possibility. The flexibility one has in tailoring the cost function to a specific application has been illustrated using broadband excitation as an example.

A 125 μs pulse was designed by changing the cost function used in our previous optimal control procedures [4, 5]. The new cost gives preference to small residual z components in the excited magnetization over residual phase in the transverse plane. This enables the algorithm to find a nearly ideal solution with a four-fold reduction in pulse length compared to the original cost, using the same peak RF. The pulse, digitized in 0.5 μs increments, has a peak RF amplitude of 17.5 kHz and is tolerant to a range of RF inhomogeneity ($\pm$0.5 dB) that is more than sufficient for high resolution NMR probes. It produces final transverse magnetization of essentially uniform phase over resonance offsets of 40 kHz. Using the same design criteria, we also derived a 125 μs pulse with significantly reduced digitization (16 time-steps, 7.8 μs per RF increment) which exhibits similar experimental performance. The pulse length of 125μs is sufficiently short that the algorithm forces the RF to its maximum allowed value of 17.5 kHz at almost all time increments, effectively generating a constant-amplitude, phase-modulated pulse.

As noted, the primary objective of this work is the continued development of productive optimal control algorithms that can be applied to any application. Excitation provides a particularly simple example that allows a clear delineation between the effects of optimal control and the application, which might be less apparent with a more complicated sequence. Pulses obtained to date can be downloaded in Bruker and Varian formats from http://www.org.chemie.tu-muenchen.de/people/bulu/.]]

ACKNOWLEDGMENTS

B.L. thanks the Fonds der Chemischen Industrie and the Deutsche Forschungsgemeinschaft (Emmy Noether fellowship LU 835/1-1) for support. S.J.G. acknowledges support from the Deutsche Forschungsgemeinschaft for Grants Gl 203/3-1 and Gl 203/4-1 and the Fonds der Chemischen Industrie. N.K. would like to acknowledge Darpa Grant F49620-0101-00556. We thank K. Kobzar (TU Munich) for experimental support.

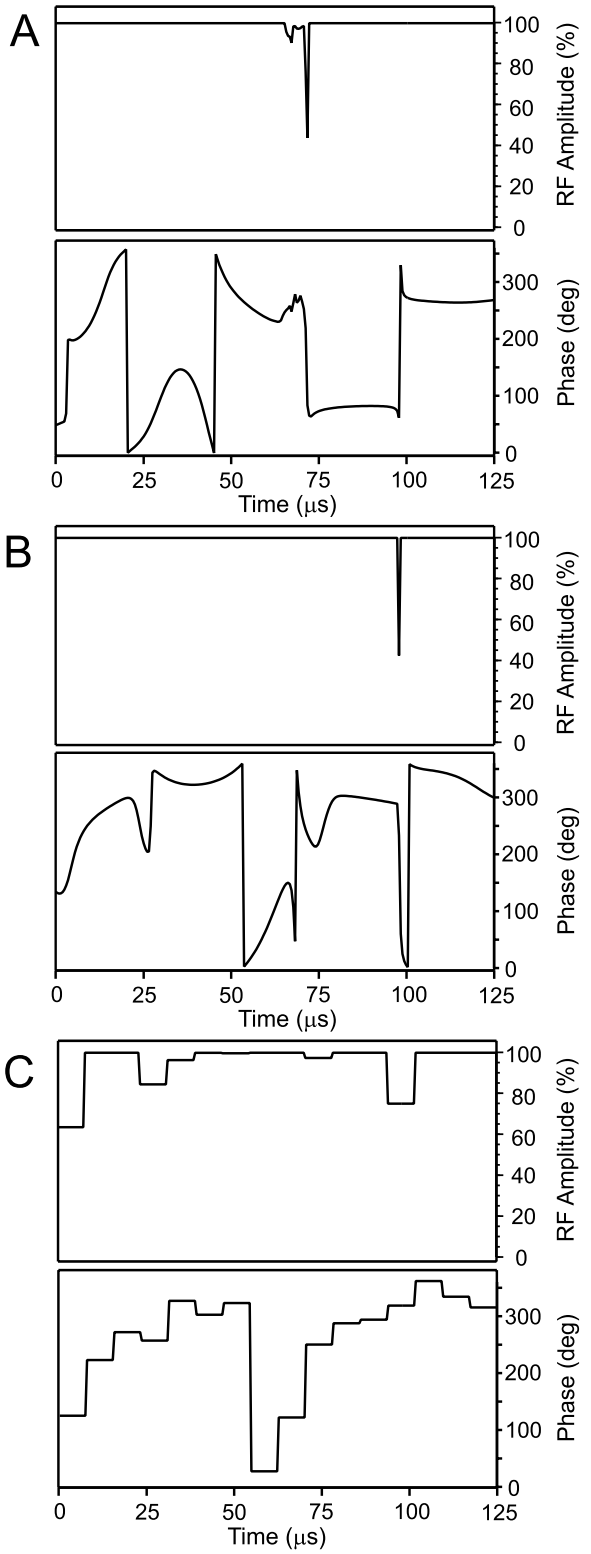

FIG. 1. Three different versions of a 125μs broadband excitation pulse, optimized to perform over resonance offsets of $\pm$20 kHz and a variation of $\pm$5% in the nominal RF calibration, are plotted as amplitude (upper panel) and phase (lower panel), illustrating the progression in their development: **(A)** a 250-point pulse derived using the original cost function $\Phi = M \cdot F$ of Refs. [4, 5] **(B)** a 250-point pulse derived using the new cost function of Eq. [6] **(C)** 16-point pulse derived using the new cost function. All three pulses provide excellent performance within the optimization window, but the best performance is given by pulse (B) ($>$ 98% excitation within 2° of the x-axis; see Fig. 2). The phase for the transverse magnetization produced by pulse (A) can be as high as 10° (see Fig. 3). Pulse (C) provides almost equal performance to pulse (B) ($>$ 97% excitation within 3° of the x-axis; see Fig. 4). The maximum RF amplitude was limited to 17.5 kHz by clipping whenever the amplitude exceeded this value, as described in [5].

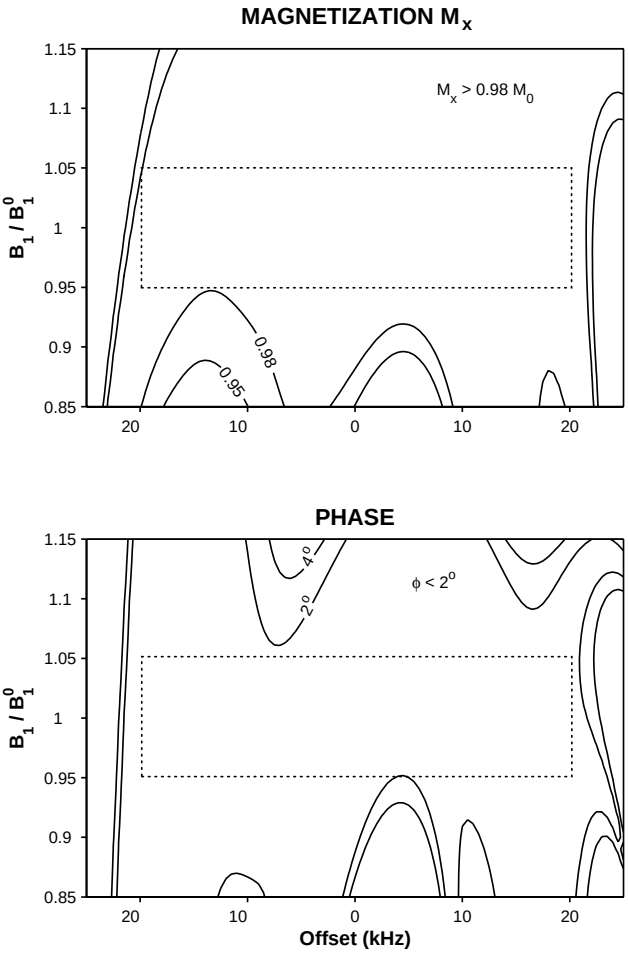

FIG. 2. Simulated performance of the optimized 125μs pulse of Fig. 1B. The dotted rectangle defines the window over which the optimization was performed. The magnitude M_x (upper panel) and phase ϕ (lower panel) of the excited magnetization is plotted as a function of resonance offset and RF field B_1, represented as a fraction of the nominal field B_1^0. Contour lines displayed for M_x are [0.98, 0.95], and those for the phase of the excited magnetization are [2°, 4°].

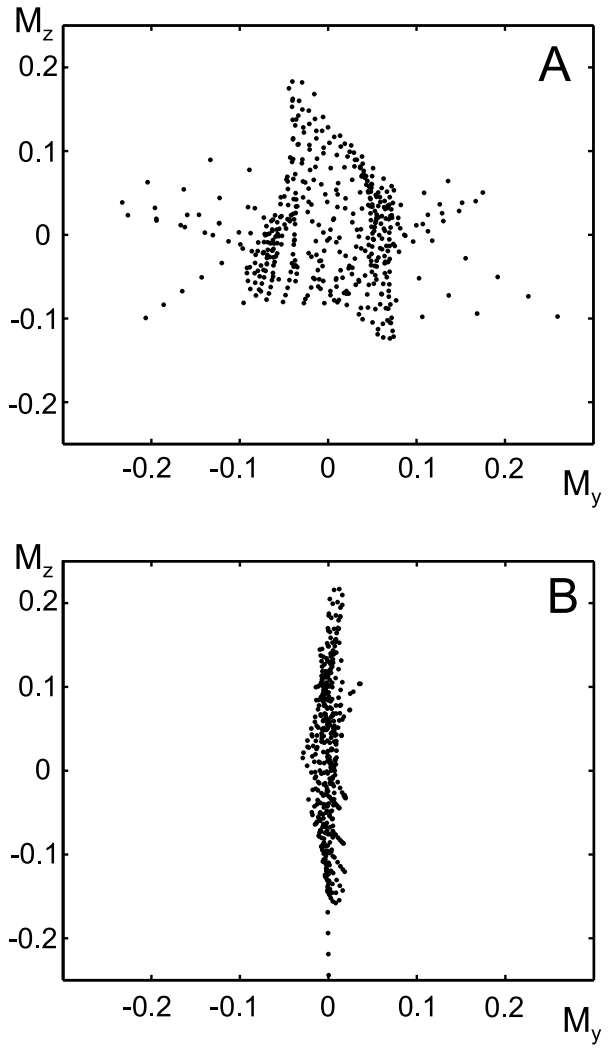

FIG. 3. Distribution of final magnetization in the y-z plane resulting from application of: **(A)** the pulse of Fig. 1A, derived using the original cost function, $M \cdot F$, and **(B)** the pulse of Fig. 1B, derived using the new cost function, Eq. [6]. The new cost produces a much narrower y distribution for the price of a small increase in width of the z distribution.

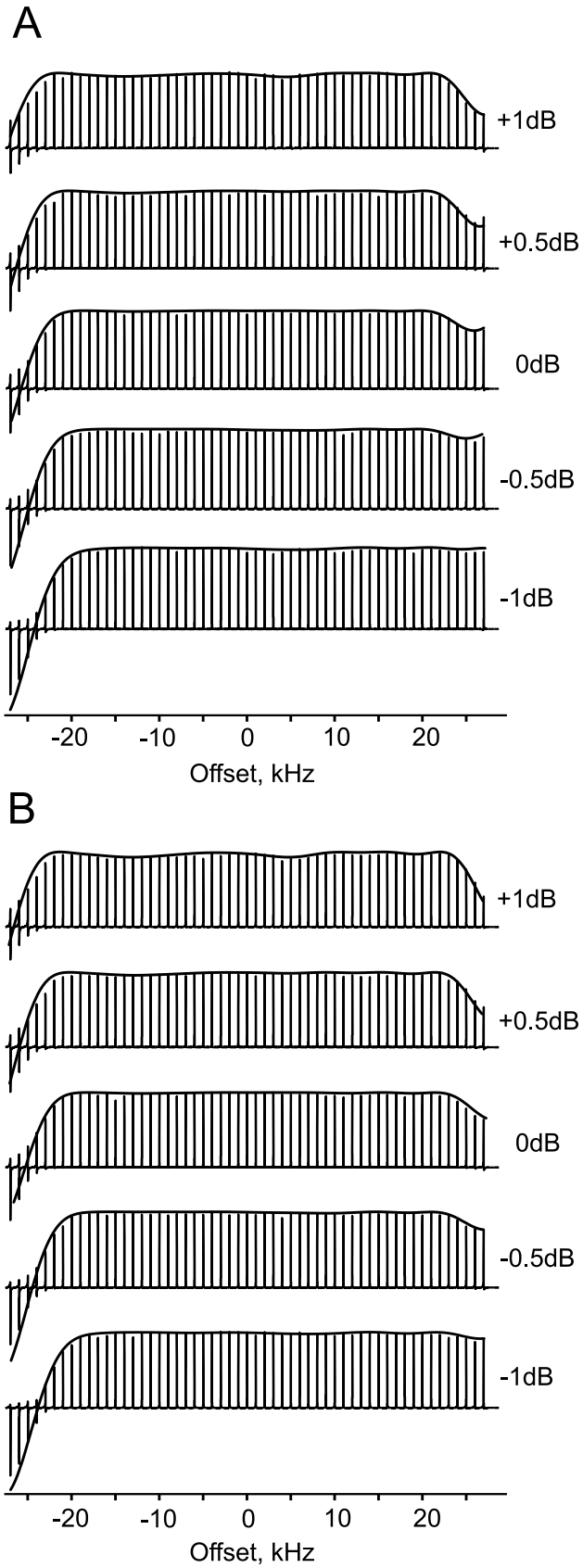

FIG. 4. Excitation profiles for the residual HDO signal in a sample of 99.96% D_2O are displayed as a function of resonance offset and RF power levels applied to the sample using **(A)** the 250-point 125 μs pulse of Fig. 1B and **(B)** the 16-point 125 μs pulse of Fig. 1C. Power levels were varied in 0.5 dB increments by adjusting attenuation relative to the calibrated pulse at 0 dB, resulting in peak RF amplitudes of 19.6 kHz (-1 dB), 18.5 kHz (-0.5 dB), 17.5 kHz (0 dB), 16.5 kHz (0.5 dB), and 15.6 kHz ($+1$ dB). The solid line at the top of each set of profiles is the theoretical performance of the pulse, plotted, as in Fig. 2, as the value of M_x after excitation of initial z magnetization, M_0. The experimental performance of both pulses is excellent, producing excitation $M_x > 0.95\,M_0$, over ± 20 kHz for RF variability within ± 1 dB $(-10.9\%, +12.2\%)$ of the calibrated value. For the $\pm 5\%$ RF variation targetted in the optimization, pulse (A) transforms $> 98\%$ of the initial z-magnetization to within 2° of the x-axis, while pulse (B) has an excitation efficiency of $> 97\%$ with phase $< 3^\circ$.

REFERENCES

1. S. Conolly, D. Nishimura, and A. Macovski, Optimal control solutions to the magnetic resonance selective excitation problem, IEEE Trans. Med. Imag. MI-5 (1986) 106–115 .
2. J. Mao, T. H. Mareci, K. N. Scott, and E. R. Andrew, Selective inversion radiofrequency pulses by optimal control, J. Magn. Reson. 70 (1986) 310–318.
3. D. Rosenfeld and Y. Zur, Design of adiabatic selective pulses using optimal control theory, Magn. Reson. Med. 36 (1996) 401–409.
4. T. E. Skinner, T. O. Reiss, B. Luy, N. Khaneja, and S. J. Glaser, Application of optimal control theory to the design of broadand excitation pulses for high resolution NMR, J. Magn. Reson. 163 (2003) 8–15 .
5. T. E. Skinner, T. O. Reiss, B. Luy, N. Khaneja, and S. J. Glaser, Reducing the duration of broadband excitation pulses using optimal control with limited RF amplitude, J. Magn. Reson. 167 (2004) 68–74.
6. K. Kobzar, T. E. Skinner, N. Khaneja, S. J. Glaser, and B. Luy, Exploring the limits of broadband excitation and inversion pulses, J. Magn. Reson. (2004, in press).
7. R. Freeman, S. P. Kempsell, and M. H. Levitt, Radiofrequency pulse sequences which compensate their own imperfections, J. Magn. Reson. 38 (1980) 453–479 .
8. M. H. Levitt, Symmetrical composite pulse sequences for NMR population inversion. I. Compensation of radiofrequency field inhomogeneity, J. Magn. Reson. 48 (1982) 234–264 .
9. M. H. Levitt and R. R. Ernst, Composite pulses constructed by a recursive expantion procedure, J. Magn. Reson. 55 (1983) 247–254.
10. R. Tycko, H. M. Cho, E. Schneider, and A. Pines, Composite pulses without phase distortion, J. Magn. Reson. 61 (1985) 90–101.
11. M. H. Levitt, Composite pulses, Prog. Nuc. Magn. Reson. Spectrosc. 18 (1986) 61–122.
12. A. J. Shaka and A. J. Pines, Symmetric phase-alternating composite pulses, J. Magn. Reson. 71 (1987) 495-503.
13. J.-M. Böhlen, M. Rey, and G. Bodenhausen, Refocusing with chirped pulses for broadband excitation without phase dispersion, J. Magn. Reson. 84 (1989) 191–197.
14. J.-M. Böhlen and G. Bodenhausen, Experimental aspects of chirp NMR spectroscopy, J. Magn. Reson. Series A 102 (1993) 293–301.
15. D. Abramovich and S. Vega, Derivation of broadband and narrowband excitation pulses using the Floquet Formalism, J. Magn. Reson. Series A 105 (1993) 30–48.
16. Ē. Kupče and R. Freeman, Wideband excitation with polychromatic pulses, J. Magn. Reson. Series A 108 (1994) 268–273.
17. K. Hallenga and G. M. Lippens, A constant-time ^{13}C–^{1}H HSQC with uniform excitation over the complete ^{13}C chemical shift range, *J. Biomol. NMR* 5 (1995) 59-66.
18. T.-L. Hwang, P. C. M. van Zijl, and M. Garwood, Broadband adiabatic refocusing without phase distortion, J. Magn. Reson. 124 (1997) 250–254.
19. K. E. Cano, M. A. Smith, and A. J. Shaka, Adjustable, broadband, selective excitation with uniform phase, J. Magn. Reson. 155 (2002) 131-139.
20. L. Pontryagin, B Boltyanskii, R. Gamkrelidze, and E. Mishchenko, The Mathematical Theory of Optimal Processes, Wiley-Interscience, New York, 1962.
21. A. P. Sage, Optimum Systems Control, Prentice-Hall, Inc., Englewood Cliffs, N.J., 1968.
22. A. Bryson, Jr. and Y.-C. Ho, Applied Optimal Control, Hemisphere, Washington, D.C., 1975.
23. E. Pinch, Optimal Control and the Calculus of Variations, Oxford University Press, Oxford, 1993.
24. H. Goldstein, Classical Mechanics, Addison-Wesley, Reading, MA, 1980.